Supplemental information

Structure of the gel phase of diC22:1PC lipid bilayers determined by x-ray diffraction

John F. Nagle, Nathaniel Jennings, Weiheng Qin, Daniel Yan, Stephanie Tristram-Nagle, and Frank Heinrich

Supplemental Information for

Structure of the Gel Phase of diC22:1PC Lipid Bilayers Determined by X-ray Diffraction

John F. Nagle,[1] Nathaniel Jennings,[1] Weiheng Qin,[1] Daniel Yan,[1] Stephanie Tristram-Nagle,[1] and Frank Heinrich[1,2]

[1]Department of Physics, Carnegie Mellon University, Pittsburgh, PA USA 15213
[2]Center for Neutron Research, National Institute of Standards and Technology, Gaithersburg, MD USA 20899

I. Phase behavior and the subgel phase

A sample incubated at 5 °C was rapidly transferred on a cold pack to the X-ray sample chamber held at 5 °C. The left side of Fig. S1 shows lamellar orders up to h=14 that indexed well to a lamellar repeat spacing $D = 72.6$ Å in the z direction perpendicular to the bilayers. More dramatic was the wide angle pattern that comes from order in the in-plane r directions as shown on the right side of Fig. S1. While gel phases generally have strong scattering from the hydrocarbon chains that occurs in the range $q_r \sim 1.3$ to 1.6 Å^{-1}, only subgel phases have the weaker Bragg rods seen at smaller q_r in Fig. S1 (1), so we call this the S phase of diC22:1PC.

The temperature was subsequently increased in steps to 8 °C, 10 °C and 12 °C without a notable change in the x-ray pattern. However, at T=13 °C, a second set of peaks with orders h=1-5, corresponding to $D = 68.6$ Å, appeared in coexistence with the S peaks. We identify these peaks as belonging to the fluid F phase because these are the peaks that ultimately remained upon melting the sample. At T = 13 °C, the relative intensities of the lamellar h-orders of the F phase were considerably smaller than those of the S phase, although the ratios varied depending upon which part of the sample was exposed to x-rays as the sample was moved laterally in the beam. Also, the D spacing of the F peaks varied systematically as the relative humidity was varied. We then expected the complete transition to occur upon small additional increases in temperature above 13 °C. Instead, the relative intensities of the two phases remained the same as temperature was gradually increased. Only when the temperature was increased from T=15 °C to T=16 °C did the S

peaks all disappear, leaving only F peaks, which were all uniformly much more intense than they had been at 13 °C.
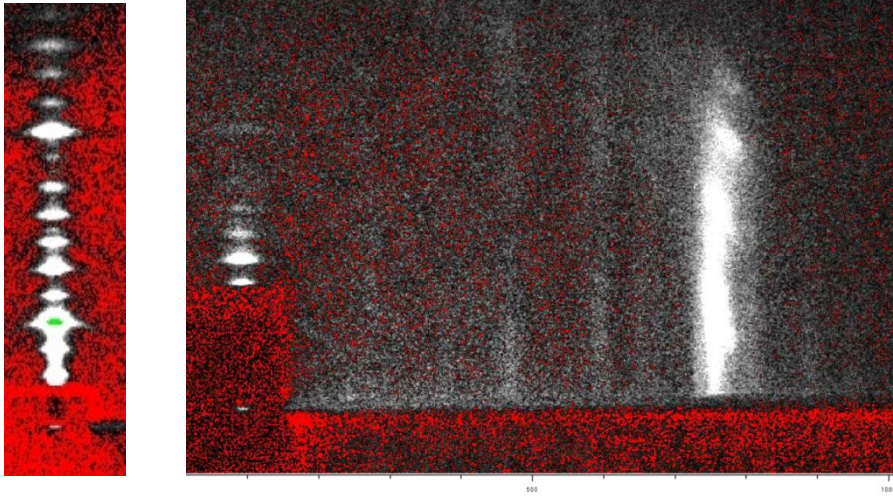

Fig. S1. Scattering from diC22:1PC bilayers in the S phase with background instrumentally subtracted. White pixels show high intensity. Red pixels indicate negative values after background subtraction. The left side shows lamellar orders h=2-14 in the q_z direction, taken while the sample was rotated in the beam; these give $D = 72$ Å. The right side was taken with the beam incident on the sample at the fixed angle of 0.5º with the very intense h=1-4 lamellar orders covered by the beam stop. In-plane scattering consists of Bragg rods at fixed q_r and variable q_z. The most intense WAXS scattering occurs on the Bragg rod at $q_r = 1.42$ Å^{-1}. Several additional weaker Bragg rods can also be discerned at $q_r = 0.41$, 0.65, 0.83, 1.1, 1.2, 1.45 and 1.7 Å^{-1}. Data were collected using a rotating anode.

The temperature was then lowered below $T = 13$ °C. The ensuing WAXS scattering pattern in Fig. 2 in the main text is considerably different from that in Fig. S1, and the intensities of the lamellar orders are also quite different as quantified in Fig. S2. Figure 2 shows two Bragg rods but no intermediate Bragg rods, so we call that the gel phase. As is also shown in Fig. S2, both ordered phases have stronger higher orders than the F phase; that is well understood as due to the smaller bending modulus of the F phase dispersing the intensity of the lamellar orders into diffuse scattering (2). Even after 3 days at $T = 11$ ° C, the S phase did not reappear. This is consistent with the nucleation and growth model that has been shown to apply to the DPPC subgel phase (3,4). To nucleate S domains within the experimenters' patience window, it is necessary to cool by an amount ΔT_S substantially below T_S. In the case of DPPC, ΔT_S is about six degrees (3). In the case of DiC22:1PC, we can only say that ΔT_S is between 3 °C and 8 °C because the subgel phase did not form at $T = 10$ °C, and 8 ° C because it did form at 5 °C, although only

after a long time. We conclude that a small portion of our original sample was in this ordinary low-temperature gel (G) phase that we subsequently showed does melt at the reported main transition at $T_M = 13$ °C and that most of the sample was originally in a subgel S phase that melted only at a temperature T_S higher than 15 °C. This implies that the S phase is the stable one below T_S and that the G phase is metastable at all temperatures. Fig. S3 shows qualitative free energy curves for this behavior.
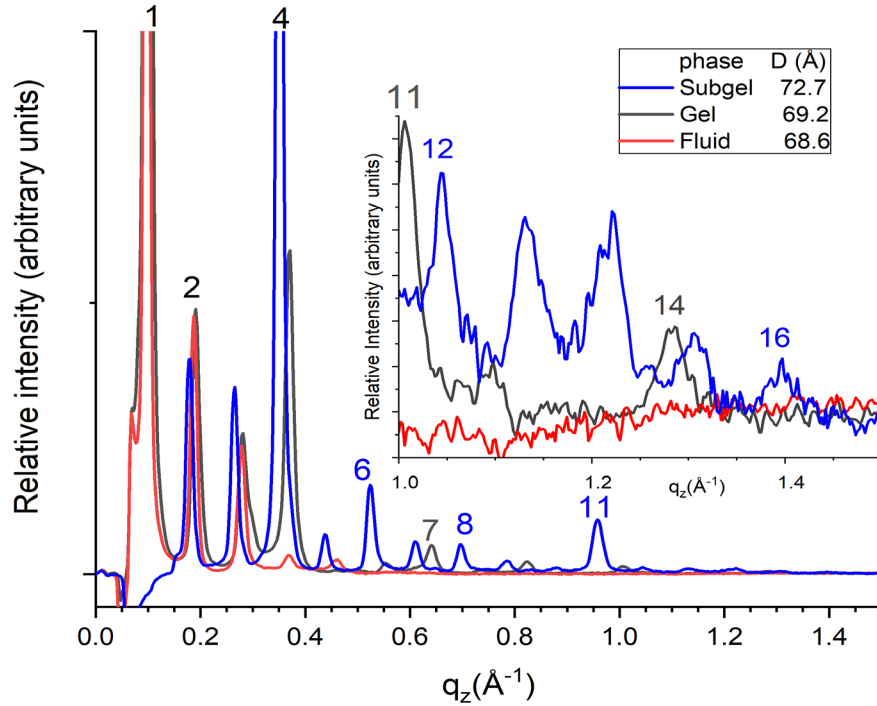

Fig. S2. Comparison of relative intensities of three phases, subgel, gel and fluid, with D spacings indicated in the legend. Some peak orders are marked by numbers h, denoting the order for the phases with higher order numbers color coded as indicated in the legend. The fluid phase intensities in red rapidly become much weaker as order h increases. The intensities of the gel and subgel are quite strong to much higher order, even before the Lorentz correction facto proportional to h.
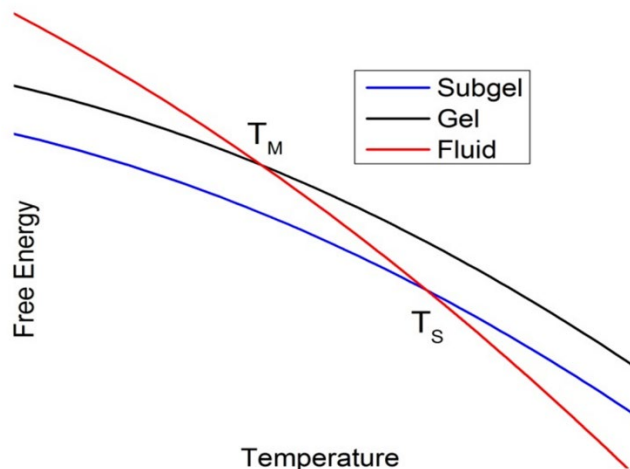
Fig. S3. Qualitative free energies of the three phases in this paper. The initial subgel phase melted into the fluid phase at $T_S \approx 16$ ºC. Upon cooling, the fluid phase transformed into the gel phase at $T_M = 13$ ºC. This thermal behavior is consistent with the sketch in which the gel phase is metastable to the subgel phase below T_M. A similar interpretation was proposed for the phase behavior of a different lipid (5).

II. Determination of intensities of weak peaks near strong peaks
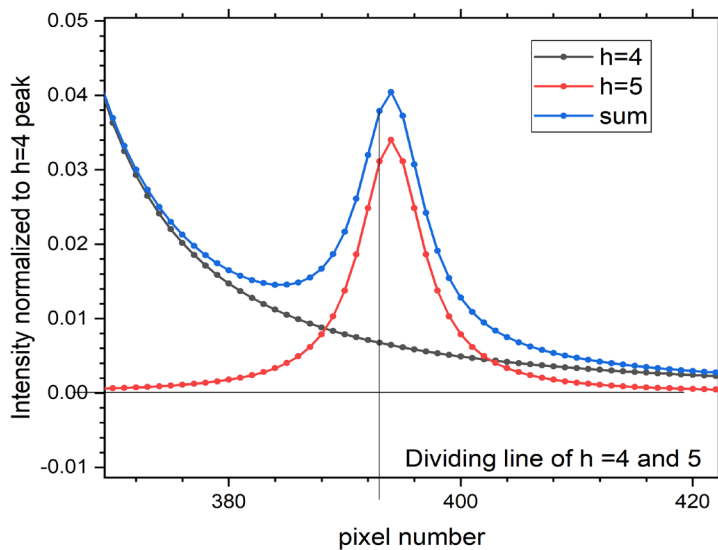

Fig. S4. The black curve is the tail of a Lorentzian with peak intensity 1.0 at pixel 353. The red curve is a Lorentzian for a weaker (h=5) peak. The true intensity of the weak peak is obtained by integrating the total intensity (blue) from the black line to higher pixel number. Integrating from the midpoint (at pixel 373) between the two peaks would more than double the h=5 intensity. Even integrating from the minimum of the blue curve would be a considerable overestimate.

III.   Comparison of electron density profiles of DPPC and C22:1PC gel phases.
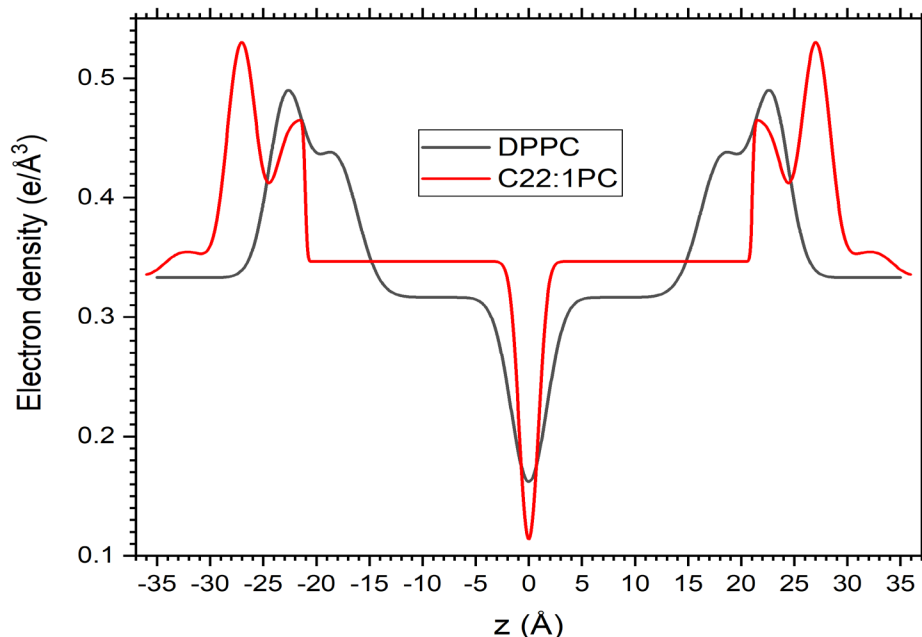

Fig. S5.   Electron density versus distance along the normal to the bilayer. The red C22:1 curve is reproduced from the sum curve in Fig. 7, which uses the model in this paper, and the black DPPC curve is reproduced from Fig. 4 in (6), which used the SDP model (7). As expected for longer chains, the headgroups are further apart for C22:1PC, and the hydrocarbon plateau is longer. Because the chains are more tightly packed, the plateau is higher for C22:1PC. In addition, the smaller headgroup peak associated with the carbonyl-glycerol moiety is more differentiated from the highest peak, which is associated with the phosphate group. Finally, the width of the terminal methyl trough in the center of the bilayer is narrower for C22:1PC, consistent with all the methyls in each bilayer occurring the same distance from the center, whereas DPPC has mini-interdigitation (6).

IV. Molecular Volume

The volume of a lipid molecule V_L was measured in fully hydrated multilamellar (MLV) vesicles using an Anton-Paar USA DMA5000M (Ashland, VA) vibrating tube densimeter with a 1:20 lipid:water mass ratio. Figure S6 shows heating and cooling scans that agree very well with each other above the phase transition. Furthermore, the molecular volume agrees very well with the molecular volume of DOPC (1303 Å^3 at $T =$ 30 ºC) (8) by adding eight methylene volumes (27.7 Å^3/methylene). In contrast, there was considerable hysteresis below the transition. We were concerned about the documented artifact incurred by the apparatus for gel phase DPPC, so we reloaded the sample many

times. However, the lipid density is close to that of water, so there was little driving force for the artifact observed in the DPPC gel phase (9).   We also investigated time dependence for gel phase formation. We tentatively used $V_L = 1478$ Å^3 at T = 10 ºC. However, that value leads to strong contradictions between the WAXS and LAXS results. We then performed diffraction on oriented MLVs and found that the LAXS intensities were inconsistent with those shown in Fig. 4 for oriented stacks. We have concluded that MLVs and oriented stacks have different structures due to curvature incompatibility discussed in the text. Since we have no method to measure V_L for oriented stacks, the analysis in the text estimates it from the measured chain volume and an estimate of the head group volume.
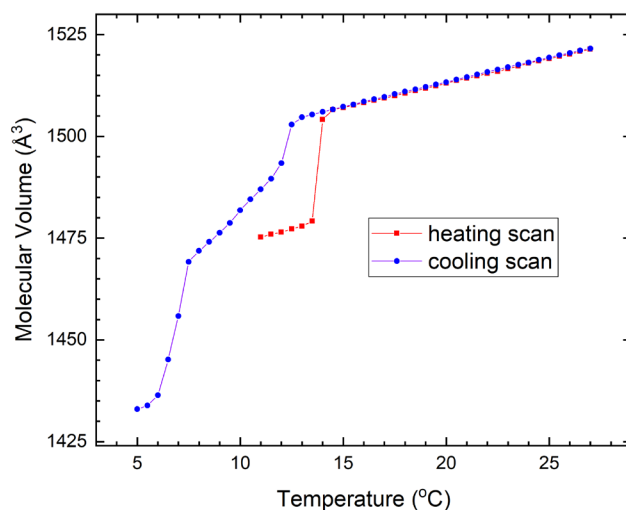

Fig. S6. Heating and cooling scans of molecular volume.

Bibliography

1.   Raghunathan, V. A., and J. Katsaras. 1995. Structure of the L(C') Phase in a Hydrated Lipid Multilamellar System. *Phys Rev Lett*. 74(22):4456-4459, <Go to ISI>://A1995QZ97000025.
2.   Zhang, R. T., R. M. Suter, and J. F. Nagle. 1994. Theory of the Structure Factor of Lipid Bilayers. *Phys Rev E*. 50(6):5047-5060, <Go to ISI>://A1994QA10800087.
3.   Yang, C. P., and J. F. Nagle. 1988. Phase-Transformations in Lipids Follow Classical Kinetics with Small Fractional Dimensionalities. *Phys Rev A*. 37(10):3993-4000, <Go to ISI>://A1988N467000040.

4.   Tristramnagle, S., R. M. Suter, W. J. Sun, and J. F. Nagle. 1994. Kinetics of Subgel Formation in Dppc - X-Ray-Diffraction Proves Nucleation-Growth Hypothesis. *Biochimica Et Biophysica Acta-Biomembranes*. 1191(1):14-20, <Go to ISI>://A1994NH54600003.

5.   Wilkinson, D. A., and J. F. Nagle. 1984. Metastability in the Phase-Behavior of "Dimyristoylphosphatidylethanolamine Bilayers. *Biochemistry-Us*. 23(7):1538-1541, <Go to ISI>://A1984SK48400030.

6.   Nagle, J. F., P. Cognet, F. G. Dupuy, and S. Tristram-Nagle. 2019. Structure of gel phase DPPC determined by X-ray diffraction. *Chem Phys Lipids*. 218:168-177, doi: 10.1016/j.chemphyslip.2018.12.011, <Go to ISI>://WOS:000459519000020.

7.   Kucerka, N., J. F. Nagle, J. N. Sachs, S. E. Feller, J. Pencer, A. Jackson, and J. Katsaras. 2008. Lipid bilayer structure determined by the simultaneous analysis of neutron and x-ray scattering data. *Biophys J*. 95(5):2356-2367, doi: DOI 10.1529/biophysj.108.132662, <Go to ISI>://000258473900022.

8.   Kucerka, N., S. Tristram-Nagle, and J. F. Nagle. 2005. Structure of fully hydrated fluid phase lipid bilayers with monounsaturated chains. *J Membrane Biol*. 208(3):193-202, doi: DOI 10.1007/s00232-005-7006-8, <Go to ISI>://000237193400001.

9.   Hallinen, K. M., S. Tristram-Nagle, and J. F. Nagle. 2012. Volumetric stability of lipid bilayers. *Phys Chem Chem Phys*. 14(44):15452-15457, doi: 10.1039/c2cp42595e, <Go to ISI>://WOS:000310153300024.